Intercalation of Iron(III) Hexacyano Complex in a Ni,Al Hydrotalcite-like Compound

Irene Carpani, Mario Berrettoni, Marco Giorgetti, and Domenica Tonelli*

Dipartimento di Chimica Fisica e Inorganica, Università di Bologna, Viale Risorgimento 4, 40136 Bologna, INSTM, UdR Bologna

Received: December 23, 2005

The product obtained by the intercalation of hexacyanoferrate(III) inside a Ni, Al hydrotalcite-like compound (Htlc) has been characterized using XRD, FT-IR, Raman, and XAS spectroscopy. The intercalation was carried out by anionic exchange of the originally existing chloride ions. The combined use of those techniques gave more insight on the insertion chemistry of Htlcs. Extended X-ray absorption fine structure spectra of the intercalated Htlc demonstrated that the native structure was stable during the iron complex insertion, whereas the exchange process occurred with a partial reduction of hexacyanoferrate(III). Both Raman and FT-IR spectroscopy pointed out the concomitant formation of $K_2NiFe^{II}(CN)_6$ and $KNiFe^{III}(CN)_6$. The effect of aging on the intercalated product is also addressed.

Introduction

Hydrotalcites-like compounds (Htlcs) or layered double hydroxides (LDHs) are a family of synthetic anion-exchanging minerals having the general formula $[M(II)_{1-x}M(III)_x(OH)_2]^{x+}$-$A^{n-}_{x/n}\cdot mH_2O$, with $0.22 < x < 0.33$.[1] They exhibit applications in a broad range of fields and have been used as catalysts and catalyst supports, antiacids, anion scavengers, chemical additives, removers of environmental hazards in acid mine drainage,[2,3] agents for soil decontamination, and electrode materials for batteries.[4] The general formula of Htlcs, abbreviated hereafter as M(II)/M(III)-A, allows a lot of composition variables and, consequently, it is obvious that a large number of these compounds can be synthesized. Htlcs are ionic lamellar solids with positively charged layers that are balanced by exchangeable interlayer anions. Their synthesis is generally carried out by (i) exchange of inorganic or organic anions, (ii) structure reconstruction, (iii) direct coprecipitation by addition of base to solutions containing a mixture of M(II) and M(III).[5]

The reaction of anionic exchange is generally performed to modify the chemical composition of Htlc, mainly through the intercalation of those elements that can be hardly incorporated through direct synthesis.[6] Cyanide has been shown to be easily introduced into LDH systems through intercalation of metal cyano-complexes such as ferricyanide, ferrocyanide, nitroprusside, and cobalticyanide. Thus, the behavior of complex cyanides in the presence of LDH is a matter of some importance in a number of areas.[1]

In a previous work[7] we reported the study of $Fe(CN)_6^{4-}$ intercalation kinetics into a Ni/Al−Cl. The reaction was carried out with the aim of synthesising the compound $Ni_2Fe^{II}(CN)_6$, i.e., without the presence of K^+ as countercations. Pure mixed hexacyanometalates are difficult to obtain, therefore we tried a synthetic route based on the destruction of the layered structure of the Htlc intercalated with $Fe(CN)_6^{4-}$ by keeping it in contact with a Ni^{2+} solution. We did not succeed in obtaining the desired compound since the hexacyanoferrate(II) was not exchanged as such but as the ion-pair with potassium. Moreover, we could demonstrated by X-ray and FTIR absorption spectroscopy that no partial oxidation of $Fe(CN)_6^{4-}$ ion occurs during the intercalation inside the Htlc.

Several authors[1,8−11] suggest that the intercalation of hexacyanoferrate(II) and hexacyanoferrate(III) into Mg/Al or Zn/Al LDHs may be accompanied by changes in the oxidation state of iron and in the structure of the LDH system itself. Idemura et al. observed a reduction of iron in hexacyanoferrate(III) complexes after the exchange reaction by Mössbauer spectroscopy.[12]

In this paper we report the results of a study that was carried out with the aim to give more insight into the processes occurring during the insertion of $Fe(CN)_6^{3-}$ in the interlayer of a Ni/Al−Cl Htlc. The effect of aging on the intercalated product is also addressed.

Experimental Section

Sample Preparation. The starting material Ni/Al−Cl was synthesized following the coprecipitation method described by Miyata, by using freshly boiled bi-distilled water for the preparation of the solutions and working under nitrogen atmosphere to avoid the contamination from carbon dioxide.[13] All salts were ACS reagent grade. Hydrated metal salts $AlCl_3\cdot 6H_2O$, $NiCl_2\cdot 6H_2O$, and potassium ferricyanide, $K_3Fe(CN)_6$, were used as supplied by Aldrich. The solution of NaOH 1.0 M was supplied by Merck.

The intercalation of the anion $Fe(CN)_6^{3-}$ was performed with the exchange method. About 0.4 g of Htlc was suspended in 20.0 mL of water and magnetically stirred for 2 h under a high purity nitrogen flow. Then 1.5 mL of 0.4 M $K_3Fe(CN)_6$ aqueous solution, corresponding to a $Fe(CN)_6^{3-}/Al^{3+}$ molar ratio of 2.5:1, were added; the nitrogen flow was stopped, and the reaction container was sealed in order to maintain an inert atmosphere. After definite exchange times chosen on the basis of the previous results,[7] the solids obtained were separated by centrifugation, repeatedly washed with bi-distilled water, and finally dried in an oven at 50°C, under vacuum. In the present work we report the characterization of the compound obtained after a 9h exchange reaction, because in these conditions the

* Corresponding author. Tel: +390512093667. Fax:+390512093690. E-mail address: domenica.tonelli@unibo.it.

10.1021/jp0574910 CCC: $33.50
Published on Web 04/06/2006

yield of the intercalated Htlc was the highest, as confirmed by the X-ray diffraction (XRD) patterns shown in the following.

X-ray Diffraction. X-ray powder diffraction patterns were recorded, in the 2θ range of 5−80°, on a Philips PW 1050/81 X-ray powder diffractometer equipped with a graphite monochromator and a vertical goniometer, using Cu Kα radiation (1.5406 Å) and a scanning rate of 0.05 deg/s.

FT-IR Spectra. The Fourier transform infrared spectra (FT-IR) were recorded with a Nicolet Nexus 470 spectrometer, configured with a Nicolet Continuum microscope and a MCT/B liquid-nitrogen-cooled detector. Spectra were collected in ATR (attenuated total reflectance) mode through a Cassegrain objective (14×), reaching a spatial resolution of ∼100 μm^2. The samples were investigated without any pretreatment by putting in intimate contact the silicon crystal with the powder. The spectra were recorded (as sum of 256 scans with a resolution of 4 cm^{-1}) in the spectral region of the medium infrared (500−4000 cm^{-1}).

Raman Spectra. A Renishaw Raman system RM1000 was employed to perform Raman analyses in the range between 2000 and 2500 cm^{-1}. It was configured with a Leica DMLM microscope (with 5×, 20×, 50×, and 20× LD objectives), a notch filter, and a charge-coupled device (CCD) thermoelectrically cooled (203 K) detector. An argon ion laser (514.5 nm) and a diode laser (780.0 nm) were used as radiation sources, with nominal laser power varied from 10 to 25 mW. In a typical Raman experiment, the laser was focused on the sample with the help of an objective lens; in all cases a 50× objective was employed. To obtain a satisfactory signal-to-noise ratio, the time of each scan was 10 s and the scans were from 2 to 10. Spectra were calibrated using the 520 cm^{-1} Raman line of a silicon wafer.

XAS Data Collection. X-ray absorption experiments (XAS) were performed at the Synchrotron Radiation Source (SRS) at Daresbury Laboratory, Warrington, England using the beam line 7.1. The storage ring operated at 1.6 GeV with a typical current of 240 mA. A Si (111) double crystal monochromator was employed. To reduce higher harmonics, the second crystal was detuned at about 70%. Internal references for energy calibration were used for iron and nickel. Data at the Fe K-edge were acquired in fluorescence mode using a Ge high-purity, 13-element solid-state detector, and in transmission mode at the Ni K-edge. XAS spectra were collected in the $k(Å^{-1})$ space up to $k = 15$ at 0.03 k intervals with a three second integration time allowing extended X-ray absorption fine structure (EXAFS) spectra to be recorded sequentially after the near edge X-ray absorption structure (XANES) region. Samples were prepared by mixing powdered compounds with cellulose (Merck) (20:80 w/w) and applying a pressure of about 5 tons cm^{-2} in order to obtain a pellet.

XANES spectra were normalized to an edge jump of unity. A prior removal of the background absorption was done by subtraction of a linear function extrapolated from the preedge region. The EXAFS analysis was performed using the GNXAS package[14,15] that takes into account multiple scattering (MS) theory.

Results and Discussion

Both the XRD patterns of the pristine Ni/Al−Cl and of the intercalated compound, hereafter named Ni/Al−$Fe^{III}(CN)_6$ (Figure 1), showed some diffraction maxima typical of hydrotalcite compounds at 11.1, 22.8, and 35.0 (2θ), due to diffraction by basal planes (003), (006), and (009), corresponding to d-spacings of 7.82, 3.91, and 2.61 Å, respectively. In addition,

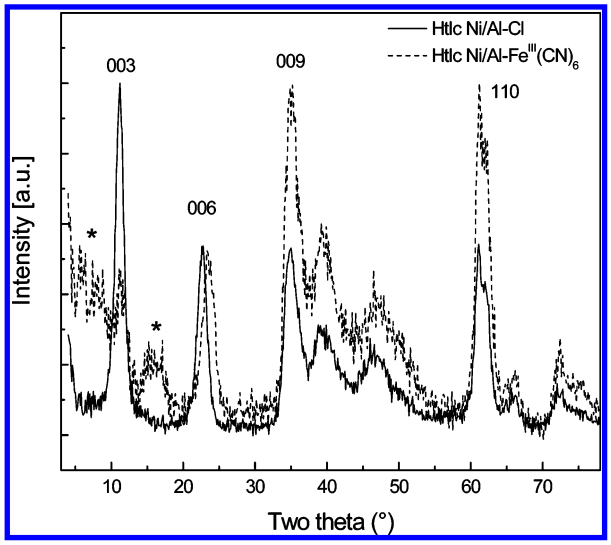

Figure 1. XRD patterns of the pristine Ni/Al−Cl and of Ni/Al−$Fe^{III}(CN)_6$.

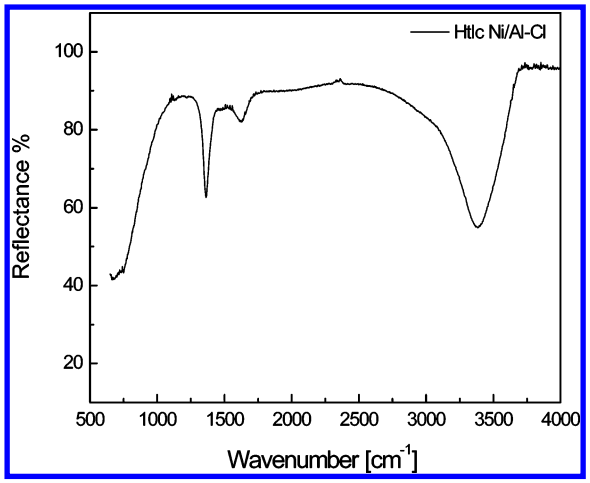

Figure 2. FT-IR spectrum of the Htlc Ni/Al−Cl.

a doublet close to 60° (2θ), where the maximum at 1.52 Å corresponds to diffraction by plane (110),[8] was observed. The crystallographic parameter c was calculated as $3d_{003}$; the resulting value was 23.4 Å, typical of a hydrotalcite containing chloride as the interlayer anion.[13]

The Htlc Ni/Al−$Fe^{III}(CN)_6$ shows two characteristic reflections (marked with an asterisk), due to diffraction by basal planes (003), (006), from which a d(003) spacing of 11.1 Å has been estimated. This value is indicative of an increased interlayer spacing, close to those reported by other authors for hexacyanoferrate-containing hydrotalcites.[7,8] Furthermore, the diffraction maxima typical of the pristine Ni/Al−Cl are still present, pointing out that a total exchange of chloride anions was not achieved.

The FT-IR spectrum of the pristine hydrotalcite Ni/Al−Cl (Figure 2) shows a broad band at high frequency (3375−3415 cm^{-1}) due to the OH stretching of water molecules and hydroxyl groups of the brucitic layers, a narrower absorption band at 1626 cm^{-1} due to δH_2O vibration of the water molecule, and a band at 1363 cm^{-1}, due to the mode ν_3 of the interlayer carbonate.[1,16]

The typical band of carbonate confirms that a small amount of this anion is present in the interlayer space, probably through adsorption from atmospheric carbon dioxide, despite the precautions taken during preparation. This fact is not surprising because of the high affinity toward this anion by Htlc.[5]

The spectra recorded in the same conditions for both

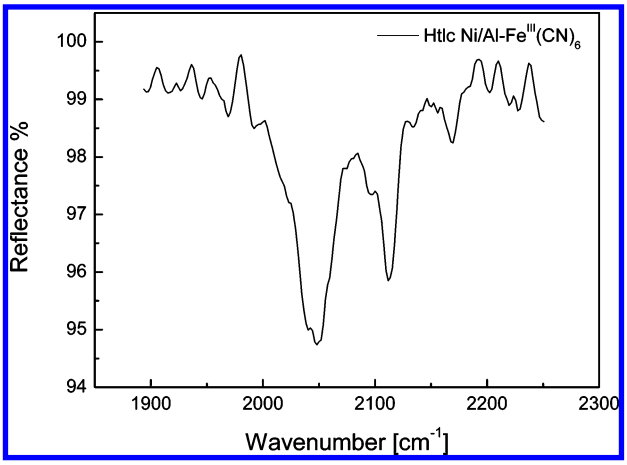

Figure 3. FT-IR spectrum of the Htlc Ni/Al−Fe^{III}(CN)$_6$.

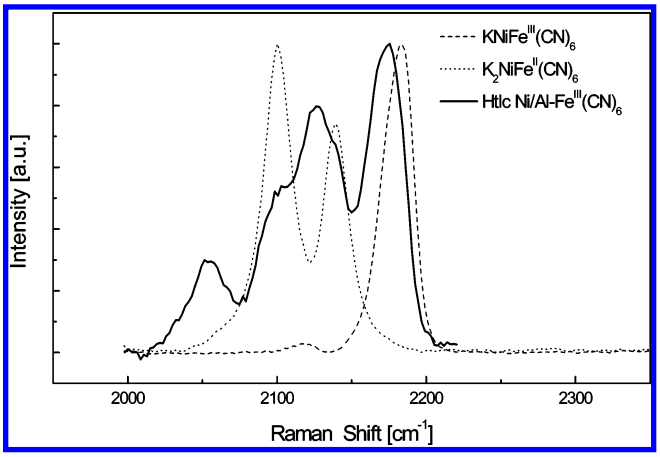

Figure 4. Raman spectra of the Htlc Ni/Al−Fe^{III}(CN)$_6$, K$_2$NiFe^{II}(CN)$_6$, and KNiFe^{III}(CN)$_6$.

hexacyanoferrate(II) and (III) in the form of potassium salts display characteristic bands due to the stretching mode ν(CN) which can be split in dependence of the crystalline state.[17] In particular, one sharp band was present at 2116 cm^{-1} in the IR spectrum of $K_3Fe(CN)_6$, whereas two strong bands at 2040 and 2021 cm^{-1}, two medium intensity bands at 2072 and 2060 cm^{-1}, and two weak bands at 2091 and 2003 cm^{-1} were recorded for $K_4Fe(CN)_6 \cdot 3H_2O$.

Figure 3 shows the IR spectrum recorded for the Ni/Al−Fe^{III}(CN)$_6$ in the range 2000−2300 cm^{-1}; two ν(CN) peaks are observed at 2168, 2113 and a splitted band at 2037−2049 cm^{-1}. From our data and literature reports,[17−19] we assigned the peak at 2113 cm^{-1} to the intercalated hexacyanoferrate(III). We attributed the splitted band at 2037−2049 cm^{-1} to the presence of hexacyanoferrate(II) formed by reduction upon intercalation.

In the IR spectrum of the intercalated Htlc, there are also two weaker peaks at 2062 and 2096 cm^{-1}, already observed for the salt $K_4Fe(CN)_6 \cdot 3H_2O$. Such a complex spectrum suggests a situation where hexacyanoferrate(II)-intercalated Htlc is in several distinct environments. Probably, due to its higher charge, hexacyanoferrate(II) has more opportunities to form hydrogen bonds with the hydrotalcite layers than hexacyanoferrate(III), making possible the observed geometrical distortions.[20] A symmetry reduction is also supported, taking into account that in the infrared spectrum the T_{1u} band splits in two bands assigned to E_u and A_{2u} components, indicating a decrease from O_h to D_{3d} symmetry.[1,9,20]

The peak at 2168 cm^{-1} was attributed to the CN stretching of the compound KNiFe^{III}(CN)$_6$ by comparison with the IR spectrum of the mixed hexacyanoferrate, synthesized by simple mixing of a soluble Ni salt and $K_3Fe(CN)_6$. As suggested by the literature,[7,21] an hypothesis explaining the formation of such a compound is that the hexacyanoferrate(III) is not incorporated as such, but as an ion-pair with potassium which interacts with nickel centers of the Htlc leading to the precipitation of a mixed hexacyanoferrate of Ni and K.

The Raman spectrum (not shown) of potassium hexacyanoferrate(II) displays two shifts at 2090 and 2062 cm^{-1}, while in the spectrum of hexacyanoferrate(III) are present a strong band at 2130 cm^{-1} and a very weak band at 2076 cm^{-1}. The shift of CN stretching from 2062 to 2130 cm^{-1} is indicative of a change in the iron oxidation state and can be explained by the decreasing π-bonding between the iron and the CN groups for hexacyanoferrate(III) compared to hexacyanoferrate(II).[5]

Figure 4 shows the Raman spectrum of the Htlc Ni/Al−Fe^{III}(CN)$_6$, in the region 2000−2300 cm^{-1}. The compound is characterized by three bands at 2056, 2127, and 2174 cm^{-1}, and two shoulders at about 2100 and 2138 cm^{-1}. In the figure are also reported the Raman spectra of the mixed hexacyanoferrates K$_2$NiFe^{II}(CN)$_6$ and KNiFe^{III}(CN)$_6$. By comparison with the bands observed for the hexacyanoferrate(III) and hexacyanoferrate(II), the Raman shifts at 2127 and around 2056 cm^{-1} indicate the presence of both cyano complexes intercalated inside the Htlc structure. Taking into account the spectra of K$_2$NiFe^{II}(CN)$_6$ and KNiFe^{III}(CN)$_6$, we ascribed the two shoulders at 2100 and 2138 cm^{-1} and the band at 2174 cm^{-1} as being due to the Fe−CN stretching when Fe(II) and Fe(III) are bonded to nickel too. The Raman data provide an additional evidence for the partial reduction of iron during the intercalation.

Similar observations for a redox process involving intercalated cyano complexes have been reported by various authors. Several studies have shown that reduction can occur under high pressure, for example during grinding.[5] However, our FTIR-ATR spectra showed a partial reduction of the Fe(III), even if any pressure was applied. Taking into account that hexacyanoferrates are known to be outer-sphere electron-transfer reductants or oxidants, Fernández et al.[22] concluded that the partial reduction took place because of the stress generated in the hexacyanoferrate(III) when it is forced to stay between the brucitic sheets of the Htlcs.

Since XRD analysis of the intercalated Htlc did not exhibit any reflections ascribable to K$_2$NiFe^{II}(CN)$_6$ and KNiFe^{III}(CN)$_6$, we hypothesized the crystalline domains were very small or the compounds were intercalated in an amorphous phase.

To check the electronic and structural modification occurred during the ferricyanide intercalation, XAS spectra were recorded. This is a powerful structural technique sensitive to short range order (a few Å around the selected atom) and can be applied to disordered, amorphous, and crystalline materials.[23] As previously demonstrated,[7] both nickel and iron local structure arrangement could be monitored before and after the hexacyanoferrate(II) ion insertion into the Ni/Al−Cl Htlc.

In this work, the structural modification has been followed either from host (Ni) and guest (Fe) sites because it should provide a more complete understanding of the entire structural dynamics, as often demonstrated by XAS.[24−26] Figure 5 shows the XANES spectra at the Ni K-edge of pristine Ni/Al−Cl Htlc and of Ni/Al−Fe^{III}(CN)$_6$ (panel a) and the XANES spectra recorded at the Fe K-edge of the Ni/Al−Fe^{III}(CN)$_6$ compared to those of hexacyanoferrate salts (panel b). Because of the relatively low concentration of iron atoms, XANES spectra of panel (b) have been recorded using fluorescence detection.

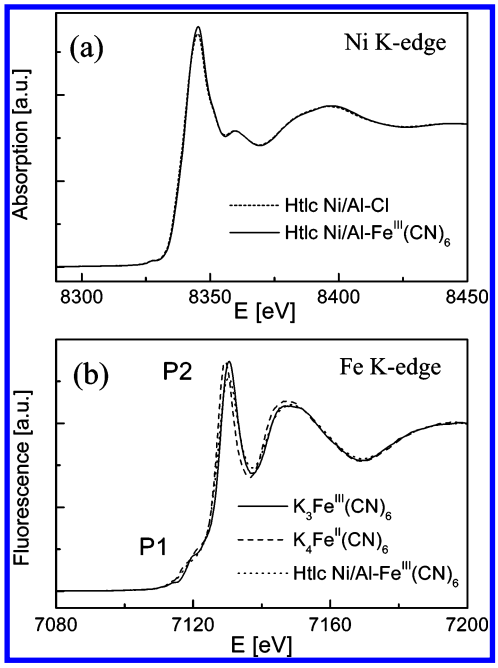

Figure 5. XANES spectra taken in transmission mode at the Ni K-edge (8333 eV, panel a) for the pristine and intercalated Htlc. XANES spectra taken with fluorescence detection at the Fe K-edge (7112 eV, panel b) for the intercalated Htlc, $K_3Fe^{III}(CN)_6$, and $K_4Fe^{II}(CN)_6$.

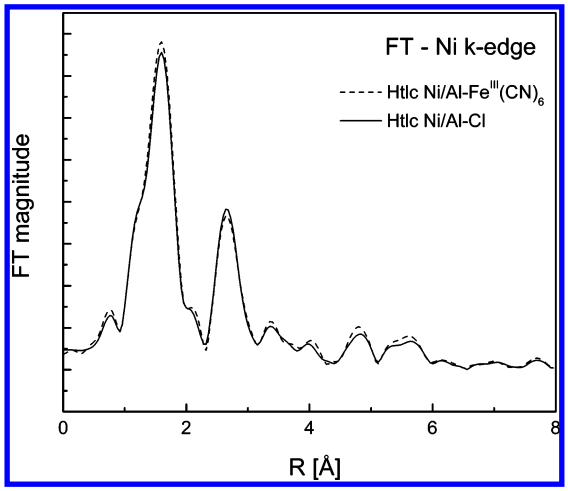

Figure 6. Experimental FT k^2-weighed EXAFS signals of the Ni/Al−Cl and Ni/Al−$Fe^{III}(CN)_6$ compounds obtained at the Ni K-edge. Hanning window in the range $k = 3.5-14.9$ Å^{-1} was used.

XANES spectra displayed in the panel (a) are almost superimposable, indicating that the local structure around the nickel (octahedrically coordinated by 6 oxygens, two in the apical position and four in the equatorial plane) has not changed. The same consideration is valid for the edge energy (threshold), thus confirming that the effective charge associated to Ni is the same. A further proof of the Htlc structure stability during hexacyanoferrates insertion, was given by the Fourier transform (FT) of EXAFS signals of the native and intercalated Htlc, which may be approximately related to the "radial distribution" around the photoabsorber (Ni) (Figure 6).

The peak, at about 1.8 Å, is due to the first coordination shell (6 oxygen); the peak at about 2.8 Å is associated to the second coordination shell, i.e., 4 Ni atoms plus 2 Al atoms. The other small peaks are due to higher coordination shells, in the single scattering approximation. It is clearly evident from the curves in Figure 6 that the local structure around Ni atoms is the same in both compounds.

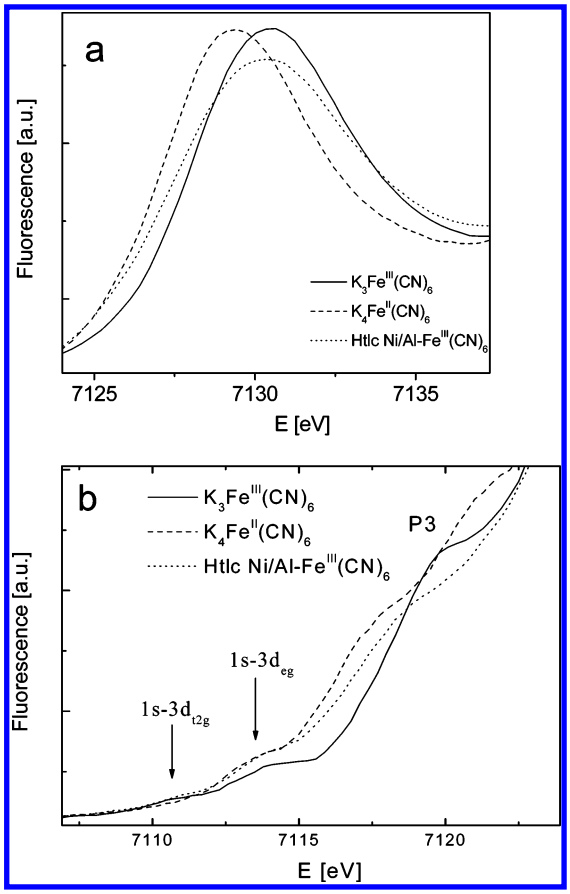

Figure 7. Details of the XANES spectra taken at the Fe K-edge (7112 eV) of the Ni/Al−$Fe^{III}(CN)_6$ compared to $K_3Fe^{III}(CN)_6$ and $K_4Fe^{II}(CN)_6$. Panel a displays the main peak, panel b the preedge area.

As pointed out in our previous publication,[7] XANES spectra were successfully used to infer on the charge associated to the iron site upon insertion of hexacyanoferrate(II) into the Htlc structure. Figure 5b reveals differences on the energy position of the main XANES features of the intercalated Htlc with respect to those of both hexacyanoferrates(II) and (III), underlying the difficulty to estimate a unique value for the iron oxidation state. However, the preedge (P1) and the main absorption edge (P2) features of Figure 5b suggest that iron in the intercalated compound is most likely in the Fe(III) oxidation state.

As shown in Figure 7a, the position of the main peak of the intercalated Htlc is close to that of the $K_3Fe^{III}(CN)_6$, even though the rising part of the spectrum is shifted toward lower energy, that is usually observed for the Fe(II) state. Figure 7b displays the magnification of the preedge region of the spectra of Figure 5b. Two small features at about 7010 and 7014 eV and the shoulder P3 can be noticed, which are present only in $K_3Fe^{III}(CN)_6$ and Ni/Al−$Fe^{III}(CN)_6$ samples. The former are due to the $1s-3d_{t2g}$ and $1s-3d_{eg}$ transitions,[27,28] the latter is associated with the transitions to empty bound states,[29] dealing with the local coordination geometry of the photoabsorber. As evident from the figure and in agreement with the literature,[30] no $1s-3d_{t2g}$ transition can be found in the $K_4Fe^{II}(CN)_6$ spectrum, since the Fe $3d_{t2g}$ level is fully occupied. Using these features, the intercalated Ni/Al−$Fe^{III}(CN)_6$ sample is consistent with Fe(III) state. Hence, XANES spectroscopy at the Fe edge indicated that the Fe formal oxidation state does not change during the intercalation of $Fe(CN)_6^{3-}$ ion in the Htlc host, even if Fe(II) could be present in isolated areas of the intercalated material. As a matter of fact, XAS is a bulk technique; therefore, a small

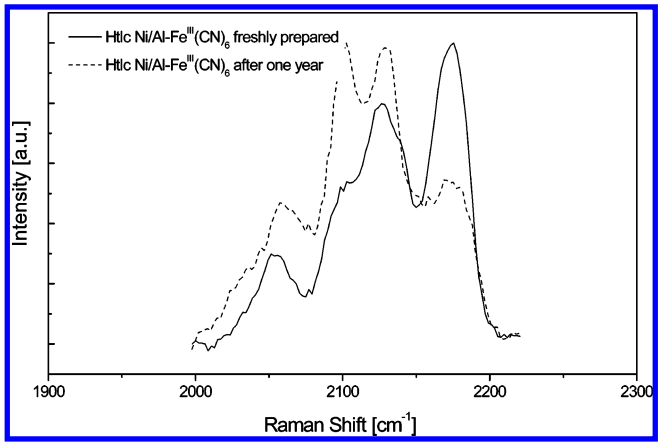

Figure 8. Raman spectra of the intercalated Htlc freshly prepared and aged for one year.

amount of Fe(II) sites is difficult to be observed if the overall concentration does not exceed 10−15% in weight.

The intercalated Htlc was aged for several months with the aim to check if the reduction of hexacyanoferrate(III) inserted in the interlayer region was time dependent. FT-IR ATR and Raman spectra were recorded. Since the changes were more evident in the Raman spectra, in Figure 8 is reported, as an example, the spectrum of the Ni/Al−$Fe^{III}(CN)_6$ recorded about one year after the synthesis. The main differences between the two spectra are ascribable to the relative intensities of the Raman shifts at about 2100 and 2174 cm^{-1}. On the basis of the assignments above-reported, the former, which is increased in intensity on aging, is due to the CN stretching of the group Fe(II)−CN−Ni, and the latter to the CN stretching of the group Fe(III)−CN−Ni. The comparison of the Raman spectra relevant to samples freshly prepared and aged for one year confirms that the reduction has continued.

Conclusions

Experimental results confirmed the intercalation of hexacyanoferrate(III) in the Htlc Ni/Al−Cl, although a total exchange of chloride anions was not achieved, as confirmed by XRD data. EXAFS spectra of the native and intercalated materials demonstrated that the Htlc structure was stable during the hexacyanoferrate insertion, while a partial reduction of iron occurred as verified by FT-IR and Raman spectroscopy, which pointed out the formation of $K_2NiFe^{II}(CN)_6$ and $KNiFe^{III}(CN)_6$. As a consequence, there is not a unique value of iron oxidation state but the intercalated hydrotalcite is characterized by a mixed-valence situation in the interlayer with both Fe(II) and Fe(III) species present. XANES spectra carried out on the Ni/Al−$Fe^{III}(CN)_6$ at the Fe K-edge were not in disagreement with this result. Furthermore, FT-IR and Raman spectra recorded approximately one year after the synthesis of the intercalated Htlc demonstrated that the extent of reduction of Fe(III) increased on aging.

Acknowledgment. Measurements at Daresbury Laboratory were supported by the European Community − Research Infrastructure Action under the FP6 "Structuring the European Research Area" Program (through the Integrated Infrastructure Initiative "Integrating Activity on Synchrotron and Free Electron Laser Science").

References and Notes

(1) Boclair, J. W.; Braterman, P. S.; Brister, B. D.; Wang, Z.; Yarberry, F. *J. Solid State Chem.* **2001**, *161*, 249.

(2) Lichti, G.; Mulcahy, J. *Chem. Australia* **1998**, *65*, 10.

(3) Seida, Y.; Nakano, Y. *J. Chem. Eng. Jpn.* **2001**, *34*, 906.

(4) Hines, D. R.; Solin, S. A. *Phys. Rev. B* **2000**, *61*, 11348.

(5) Trifirò, F.; Vaccari, A. In *Hydrotalcite-like Anionic Clays*, *Comprehensive Supramolecular Chemistry*; Alberti, G., Bein, T., Eds.; Pergamon: UK, 1996; Vol. 7.

(6) Malherbe, F.; Bigey, L.; Forano, C.; de Roy, A.; Besse, J. P. *J. Chem. Soc., Dalton Trans.* **1999**, 3831.

(7) Carpani, I.; Berrettoni, M.; Ballarin, B.; Giorgetti, M.; Scavetta, E.; Tonelli, D. *Solid State Ionics* **2004**, *168*, 167.

(8) Holgado, M. J.; Rives, V.; Sanromán, M. S.; Malet, P. *Solid State Ionics* **1996**, *92*, 273.

(9) Kloprogge, J. T.; Weier, M.; Crespo, I.; Ulibarri, M. A.; Barriga, C.; Rives, V.; Martens, W. N.; Frost, R. L. *J. Solid State Chem.* **2004**, *177*, 1382.

(10) Rives, V.; Ulibarri, M. A. *Coord. Chem. Rev.* **1999**, *181*, 61 (and references therein).

(11) Frost, R. L.; Musumeci, A. W.; Bouzaid, J.; Adebajo, M. O.; Martens, W. N.; Kloprogge, J. T. *J. Solid State Chem.* **2005**, *1787*, 1940.

(12) Idemura, S.; Suzuki, E.; Ono, Y. *Clays Clay Mineral.* **1989**, *37*, 553.

(13) Miyata, S. *Clays Clay Mineral.* **1983**, *31*, 305.

(14) Filipponi, A.; Di Cicco, A.; Natoli, C. R. *Phys. Rev. B* **1995**, *52*, 15122.

(15) Filipponi, A.; Di Cicco, A. *Phys. Rev. B* **1995**, *52*, 15135.

(16) Crespo, I.; Barriga, C.; Rives, V.; Ulibarri, M. A. *Solid State Ionics* **1977**, *101*−*103*, 729.

(17) Nakamoto, K. In *Infrared spectra of inorganic and coordination compounds*; J. Wiley & Sons: New York, 1963; p 127.

(18) Emschwiller, G. *CR Acad. Sci. Paris* **1954**, *238*, 1414.

(19) Tosi, L.; Danon, J. *Inorg. Chem.* **1964**, *3*, 150.

(20) Boclair, J. W.; Braterman, P. S.; Brister, B. D.; Yarberry, F. *Chem. Mater.* **1999**, *11*, 2199.

(21) Yao, K.; Taniguchi, M.; Nakata, M.; Shimazu, K.; Takahashi, M.; Yamagishi, A. *J. Electroanal. Chem.* **1998**, *457*, 119.

(22) Fernández, J. M.; Ulibarri, M. A.; Labajos, F. M.; Rives, V. *J. Mater. Chem.* **1998**, *8*, 2507.

(23) Filipponi, A. *J. Phys. Condens. Matter* **2001**, *13*, R23.

(24) Giorgetti, M.; Passerini, S.; Smyrl, W. H.; Berrettoni, M. *Chem. Mater.* **1999**, *11*, 2257.

(25) Giorgetti, M.; Mukerjee, S.; Passerini, S.; McBreen, J.; Smyrl, W. H. *J. Electrochem. Soc.* **2001**, *148*, A768.

(26) Frabetti, E.; Deluga, G. A.; Smyrl, W. H.; Giorgetti, M.; Berrettoni, M. *J. Phys. Chem. B* **2004**, *108*, 3765.

(27) Westre, T. E.; Kennepohl, P.; DeWitt, J. G.; Hedman, B.; Hogdson, K. O.; Solomon, E. I. *J. Am. Chem.* Soc. **1997**, *119*, 6297.

(28) Yokoyama, T.; Ohta, T.; Sato, O.; Hashimoto, K. *Phys. Rev. B* **1998**, *58*, 8257.

(29) Cecchi, P.; Berrettoni, M.; Giorgetti, M.; Gioia Lobbia, G.; Calogero, S.; Stievano, L. *Inorg. Chim. Acta* **2001**, *318*, 67.

(30) Hayakawa, K.; Hatada, K.; D'Angelo, P.; Della Longa, S.; Natoli, C. R.; Benfatto, M. *J. Am. Chem. Soc.* **2004**, *126*, 15618.